HHS Public Access

Author manuscript

Biochemistry. Author manuscript; available in PMC 2016 May 05.

Published in final edited form as:

Biochemistry. 2015 May 5; 54(17): 2709–2718. doi:10.1021/acs.biochem.5b00266.

The C-Terminal Heme Regulatory Motifs of Heme Oxygenase-2 Are Redox-Regulated Heme Binding Sites

Angela S. Fleischhacker[†], **Ajay Sharma**[§], **Michelle Choi**[†], **Andrea M. Spencer**[†,‡], **Ireena Bagai**[†], **Brian M. Hoffman**[§], and **Stephen W. Ragsdale**[†,*]

[†]Department of Biological Chemistry University of Michigan, Ann Arbor, Michigan 48109, United States

[‡]Cellular and Molecular Biology Training Program, University of Michigan, Ann Arbor, Michigan 48109, United States

[§]Department of Chemistry, Northwestern University, Evanston, Illinois 60208, United States

Abstract

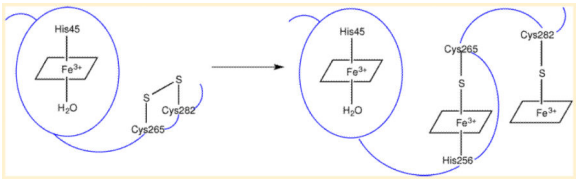

Heme oxygenase-2 (HO2), an enzyme that catalyzes the conversion of heme to biliverdin, contains three heme regulatory motifs (HRMs) centered at Cys127, Cys265, and Cys282. Previous studies using the soluble form of human HO2 spanning residues 1–288 ($HO2_{sol}$) have shown that a disulfide bond forms between Cys265 and Cys282 and that, in this oxidized state, heme binds to the catalytic site of $HO2_{sol}$ via His45. However, various mutational and spectroscopic studies have confirmed the involvement of cysteine in Fe^{3+}-heme binding upon reduction of the disulfide bond. In an effort to understand how the HRMs are involved in binding of heme to disulfide-reduced $HO2_{sol}$, in the work described here, we further investigated the properties of Fe^{3+}-heme bound to HO2. Specifically, we investigated binding of Fe^{3+}-heme to a truncated form of soluble HO2 (residues 213–288; $HO2_{tail}$) that spans the C-terminal HRMs of HO2 but lacks the catalytic core. We found that $HO2_{tail}$ in the disulfide-reduced state binds Fe^{3+}-heme and accounts for the spectral features observed upon binding of heme to the disulfide-reduced form of $HO2_{sol}$ that cannot be attributed to heme binding at the catalytic site. Further analysis revealed that while $HO2_{sol}$ binds one Fe^{3+}-heme per monomer of protein under oxidizing conditions, disulfide-reduced $HO2_{sol}$ binds slightly more than two. Both Cys265 and Cys282 were identified as Fe^{3+}-heme ligands, and His256 also acts as a ligand to the Cys265-ligated heme. Additionally, Fe^{3+}-heme binds with a

[*]**Corresponding Author** Department of Biological Chemistry, University of Michigan, 1150 W. Medical Center Dr., Ann Arbor, MI 48109. sragsdal@umich.edu. Telephone: (734) 615-4621. Fax: (734) 763-4581..

The authors declare no competing financial interest.

Supporting Information ^{14}N and ^{15}N DAVIES ENDOR spectra of unlabeled and ^{15}N-labeled Fe^{3+}-HO2 measured at various *g* values. This material is available free of charge via the Internet at http://pubs.acs.org.

much weaker affinity to Cys282 than to Cys265, which has an affinity much weaker than that of the His45 binding site in the catalytic core. In summary, disulfide-reduced HO2 has multiple binding sites with varying affinities for Fe^{3+}-heme.

Heme is an iron-containing cofactor that is necessary for a variety of cellular processes. However, because heme can also be cytotoxic, heme levels must be carefully regulated. One mechanism that contributes to the achievement of proper heme homeostasis is the heme degradation pathway. The pathway involves two enzymatic steps: the conversion of heme to biliverdin and the subsequent conversion of biliverdin to the more readily excreted product bilirubin.[1] The first, and rate-limiting, step is catalyzed by heme oxygenase (HO). HO is the only known mammalian enzyme capable of degrading heme, suggesting a vital role of HO in maintaining proper heme homeostasis.

Two major isoforms of HO have been identified in mammalian cells: heme oxygenase-1 (HO1) and heme oxygenase-2 (HO2).[2] Human HO1 is a 288-amino acid, inducible protein with particularly high levels in the liver and spleen, while human HO2 is a 316-amino acid protein that is constitutively expressed and has primarily been identified in the brain and testes.[1] Despite the differences in expression and regulation, HO1 and HO2 degrade heme with similar catalytic efficiencies[2] and share a high degree of homology (55% identical and 76% similar for the human proteins). Further, HO1 and HO2 are both tethered to the endoplasmic reticulum with similar C-terminal membrane-spanning regions comprised of 20 hydrophobic amino acids.[3]

Fe^{3+}-heme binds similarly to HO1 and HO2 in the catalytic regions near the N-termini. Both proteins adopt an α-helical fold in this region of the protein (approximately residues 1–230 of HO1 and residues 28–248 of HO2) that encompasses the heme binding site.[4,5] The imidazole nitrogen of a conserved histidine (His25 in HO1, His45 in HO2) acts as the proximal Fe^{3+}-heme iron axial ligand. On the distal side, the Fe^{3+}-heme iron interacts with a glycine-rich helix through an aquo (H_xO) ligand.

Differences in Fe^{3+}-heme binding between HO1 and HO2, however, appear to emerge upon reduction of a disulfide bond in HO2. While HO1 does not contain any cysteine residues, HO2 contains three (Cys127, Cys265, and Cys282). Cys265 and Cys282 are located in the region between the catalytic core and the membrane-spanning region, where HO2 and HO1 sequences significantly diverge. Previous studies have demonstrated the ability of Cys265 and Cys282 to form a disulfide bond with a midpoint reduction potential of −200 mV for the thiol/disulfide conversion.[6,7] Further, the thiols of Cys265 and Cys282 were shown to be 60–70% reduced under normal growth conditions, with a higher or lower percentage of reduced thiols observed under reducing or oxidative stress conditions, respectively.[6] Thus, it appears as though the thiol/disulfide conversion is physiologically relevant.

The relevance of the thiol/disulfide conversion to HO2 function and structure appears to relate to Fe^{3+}-heme binding. In particular, cysteine has been suggested to coordinate to the Fe^{3+}-heme in the disulfide bond-reduced, i.e., the dithiolate, form of HO2 (here termed $HO2^R$) but not in the disulfide form (here termed $HO2^O$).[7] While stable coordination of the cysteines to Fe^{3+}-heme has been questioned,[8] there is mounting evidence from mutational

and spectroscopic studies confirming the involvement of cysteine, Cys265 in particular, in binding of Fe^{3+}-heme to $HO2^R$.[7,9,10]

Participation of the cysteines of HO2 in Fe^{3+}-heme binding was not completely unexpected because each of the three cysteines of HO2 is found in heme regulatory motifs (HRMs), short amino acid stretches containing a Cys-Pro dipeptide that have been implicated in heme binding. While not all HRMs necessarily bind heme, a growing number of proteins containing HRMs have been found to bind Fe^{3+}-heme with varying affinity at the HRM sites via the cysteine residue. Heme binding to the HRMs has been shown in some instances to modulate the activity of the respective protein, including iron regulatory protein 2 (IRP2),[11] bacterial iron response regulator protein (Irr),[12,13] and heme-regulated eukaryotic initiation factor 2α [heme-regulated inhibitor (HRI)].[14,15] Therefore, it is not unreasonable to hypothesize that the HRMs of HO2 are involved in regulating HO2 function because HRM1, centered at Cys265-Pro266, and possibly HRM2, centered at Cys282-Pro283, appear to be involved in Fe^{3+}-heme binding.[7,9,10]

To understand if and how the HRMs affect HO2 activity, further investigation into how the HRMs of $HO2^R$ bind Fe^{3+}-heme is warranted. One hypothesis previously offered includes a "fishhook" mechanism in which a cysteine residue from one of the HRMs of $HO2^R$ displaces one of the ligands (His45 or aquo) of Fe^{3+}-heme bound to the catalytic core upon reduction of the disulfide bond.[7] Further, the same report offered the observation that $HO2^R$ bound Fe^{3+}-heme more weakly than $HO2^O$, suggesting a direct mechanism by which the HRMs could be involved in modulating the activity of HO2. Alternatively, Maines and co-workers have proposed that the HRMs form a Fe^{3+}-heme binding site that is independent of the catalytic site.[16] Indeed, Fe^{3+}-heme bound to HO2 at the catalytic site is securely sandwiched between two helices,[4] challenging the fishhook mechanism from a structural perspective. Also consistent with a multiple-binding site model is a recent spectroscopic study of HO2.[9] The intensity of the electron paramagnetic resonance (EPR) signal associated with Fe^{3+}-heme binding at the catalytic core in $HO2^O$ was shown to remain constant in $HO2^R$ rather than decreasing, which would be expected for conversion of the Fe^{3+}-heme from His45/aquo to His45/Cys ligation with the fishhook mechanism. Instead, a new signal consistent with a Cys-ligated heme appeared on top of the signal for the His45/aquo-ligated Fe^{3+}-heme, suggesting an independent binding site with Cys ligation.

In this study, we investigated the involvement of the HRMs in the binding of Fe^{3+}-heme to $HO2^R$. The soluble form of HO2 spanning residues 1–288 ($HO2_{sol}$) and a truncated variant of $HO2_{sol}$ spanning residues 213–288 ($HO2_{tail}$), which contains Cys265 and Cys282 but lacks the catalytic core, were used in this study. Spectral analyses, including absorption, EPR, and electron nuclear double resonance (ENDOR) spectroscopies, of $HO2_{tail}$ and $HO2_{sol}$ as well as variants of these proteins confirm multiple binding sites on $HO2^R$ and allowed us to identify the Fe^{3+}-heme ligands. Further, binding affinities were determined for each of the binding sites. In summary, the results presented here confirm a multiple-binding site model for $HO2^R$ in which Fe^{3+}-heme binds to the catalytic core and, independently, to the HRMs in the C-terminal tail of $HO2^R$.

METHODS

Protein Expression and Purification

The soluble form of human HO2 spanning residues 1–288 ($HO2_{sol}$) was expressed from the pET28a vector in BL21(λDE3) cells using growth conditions described previously.[9] $HO2_{sol}$ with an N-terminal six-His tag was purified on a Ni-nitrilotriacetic acid affinity column (Qiagen) before the affinity tag was removed by treatment with thrombin as described previously[9] to yield untagged $HO2_{sol}$ in the apo form with a disulfide bond (here termed $HO2_{sol}^{O}$). The soluble form of human HO2 spanning residues 1–248 ($HO2_{core}$) was constructed using the QuikChange site-directed mutagenesis protocol (Stratagene) to introduce a stop codon at amino acid 249 in pET28a/$HO2_{sol}$. After the change had been confirmed via sequence analysis, $HO2_{core}$ was expressed and purified as described for $HO2_{sol}$. The soluble form of human HO2 spanning residues 213–288 ($HO2_{tail}$) was cloned by ligation-independent cloning[17] into a modified version of expression vector pMCSG7[18] containing the protein G B1 domain (GB1) to enhance solubility[19] (modified vector generously provided by W. C. Brown of the High-throughput Protein Lab in the Center for Structural Biology at the University of Michigan). GB1-$HO2_{tail}$ with an N-terminal six-His tag was expressed and purified on a Ni-nitrilotriacetic acid affinity column as described for $HO2_{sol}$ except that tobacco etch virus protease was used to cleave the protein at a cleavage site between the GB1 domain and $HO2_{tail}$, as described previously,[20] to yield the apo form of $HO2_{tail}$. Variants of $HO2_{tail}$ were constructed using the QuikChange site-directed mutagenesis protocol (Stratagene) to introduce point mutations, and variants were expressed and purified as described for wild-type $HO2_{tail}$.

Preparation and Analysis of Fe^{3+}-Heme Bound HO2

$HO2_{sol}^{O}$ and $HO2_{tail}^{O}$ were treated with a 25-fold molar excess of tris(2-carboxyethyl)phosphine (TCEP) for 1 h in an anaerobic chamber. The proteins were passed through two successive Micro Bio-Spin 6 columns (Bio-Rad) that had been pre-equilibrated in anaerobic buffer A [50 mM Tris buffer (pH 8.0) containing 50 mM KCl] to remove TCEP. The disulfide-reduced proteins (here termed $HO2_{sol}^{R}$ and $HO2_{tail}^{R}$) were then incubated for 1 h in the anaerobic chamber with a 5-fold molar excess of Fe^{3+}-heme. The Fe^{3+}-heme stock was freshly prepared in anaerobic buffer A with 15% dimethyl sulfoxide and 0.1 M NaOH. The stock was passed through a 22 μm filter to remove insoluble matter, and the concentration was determined by using an ε_{385} of 58.4 mM^{-1} cm^{-1}.[21] After the incubation time, the protein/Fe^{3+}-heme mixture was removed from the anaerobic chamber and subsequently passed through a PD-10 desalting column (GE Healthcare), which separated out unbound heme from the Fe^{3+}-heme-bound proteins (here termed Fe^{3+}-$HO2_{sol}^{R}$ and Fe^{3+}-$HO2_{tail}^{R}$). The Fe^{3+}-heme-bound forms of $HO2_{sol}^{O}$ and $HO2_{core}$ (Fe^{3+}-$HO2_{sol}^{O}$ and Fe^{3+}-$HO2_{core}$, respectively) were prepared as described above except without TCEP treatment prior to incubation with Fe^{3+}-heme, and all steps were conducted under aerobic conditions.

Absorbance spectra of the Fe^{3+}-heme-bound proteins were recorded at a protein concentration of 5 μM in buffer A at 20 °C on a Shimadzu UV-2600 UV–vis spectrophotometer. The amount of Fe^{3+}-heme bound to the proteins was quantified with the

pyridine hemochrome assay using a difference extinction coefficient at 556 nm of 28.32 mM^{-1} cm^{-1}.[22] EPR samples were prepared at a protein concentration of 100 μM in buffer A, and spectra were recorded on a Bruker EMX spectrometer equipped with an Oxford ITC4 temperature controller, a Hewlett-Packard model 5340 automatic frequency counter, and a Bruker gaussmeter. Measurements were performed at 10 K with a microwave power of 2 mW, a microwave frequency of 9.39 GHz, a modulation amplitude of 10.15 G, and a modulation frequency of 100 kHz.

ENDOR Spectroscopy

^{15}N-labeled proteins were prepared as described above except that the cells were cultured in M9 minimal medium supplemented with 1.0 g/L $^{15}NH_4Cl$. Unlabeled and ^{15}N-labeled Fe^{3+}-$HO2_{tail}^{R}$ were prepared as described above except that the apo form of the protein was concentrated and then incubated in a 1:1 ratio with Fe^{3+}-heme. Unlabeled and ^{15}N-labeled Fe^{3+}-$HO2_{sol}^{O}$ and Fe^{3+}-$HO2_{sol}^{R}$ were prepared by adding Fe^{3+}-heme to the apo form of the proteins until the ratio of the absorbance at 404 nm to that at 280 nm was constant, as described previously.[9] Glycerol was subsequently added to the samples to a final concentration of 50%. EPR and ENDOR measurements were performed at 35 GHz as described previously.[9]

Fe^{3+}-Heme Difference Titrations

$HO2_{sol}^{R}$ and $HO2_{tail}^{R}$, as well as its variants, were prepared with TCEP reduction under anaerobic conditions as described above. While in the anaerobic chamber, the proteins were diluted to the appropriate concentration in anaerobic buffer A and transferred to a serum-stoppered cuvette (sample). An equal volume of anaerobic buffer A was transferred to a second serum-stoppered cuvette (reference). Both cuvettes were titrated with small aliquots of Fe^{3+}-heme via a Hamilton syringe. The Fe^{3+}-heme stock was prepared under anaerobic conditions as described above, diluted to ~300 μM in anaerobic buffer A, and transferred to a serum-stoppered vial. The concentration of the diluted stock was confirmed as described above. Difference spectra were recorded at 20 °C in a Shimadzu UV-2600 UV–visible spectrophotometer. Difference titrations with $HO2_{core}$ were performed as described for the disulfide-reduced proteins except that the protein was not treated with TCEP prior to the experiment. The data were fit to the quadratic equation as described previously for HO2[7] in GraphPad Prism 6.

Fe^{3+}-Heme Off-Rate Measurements

Apo-H64Y/V68F-myoglobin[23] was prepared using the methyl ethyl ketone extraction method described previously[24] with protein generously supplied by J. Olson (Rice University, Houston, TX). After extensive dialysis against 50 mM Tris (pH 7.4) and 150 mM KCl, the apoprotein was centrifuged to remove precipitates. The protein concentration was determined using an extinction coefficient at 280 nm of 17 mM^{-1} cm^{-1}.[25]

In buffer A, 2 μM Fe^{3+}-heme-bound protein, prepared as described above, was mixed with 20 μM apo-H64Y/V68F-myoglobin. Spectra were recorded over time at 20 °C in a Shimadzu UV-2600 UV–visible spectrophotometer. Data were fit to either single- or double-exponential functions using GraphPad Prism 6.

Fe^{3+}-Heme On-Rate Measurements

On-rate measurements were taken using an Applied Photophysics spectrophotometer (SX.MV18 with the Pro-Data upgrade) in which the sample-handling unit of the stopped-flow instrument is within an anaerobic chamber. The optical path of the observation cell was 1 cm, and the instrument was used in photomultiplier mode at 20 °C while monitoring at 406 nm. Fe^{3+}-heme and the proteins used in these experiments [$HO2_{core}$, $HO2_{tail}(C282A)^R$, and $HO2_{sol}{}^R$] were prepared in anaerobic buffer A as described above. Each k_{obs} value represents an average of five to seven consecutive traces fit to a single-exponential equation using the Applied Photophysics software.

RESULTS

Evaluation of Binding of Fe^{3+}-Heme to $HO2^R$

$HO2_{tail}$, a construct that spans residues 213–288 of HO2 (including the two C-terminal HRMs but not the residues previously identified to be important for heme binding at the catalytic site), was investigated for its ability to bind heme. Because Cys265 and Cys282 were previously shown to form a disulfide bond,[7] $HO2_{tail}{}^O$ was treated with TCEP before being tested for its ability to bind Fe^{3+}-heme. After separation from TCEP, $HO2_{tail}{}^R$ was incubated with excess Fe^{3+}-heme, and unbound Fe^{3+}-heme was subsequently removed before further analysis. The pyridine hemochrome assay demonstrated that Fe^{3+}-$HO2_{tail}{}^R$ bound 1.4 ± 0.3 hemes per monomer of protein. Further, the absorbance spectrum of Fe^{3+}-$HO2_{tail}{}^R$ included a broad band at 368 nm and a shoulder at 422 nm (Figure 1A). The spectrum is reminiscent of spectra reported for other proteins that bind heme at HRMs, including IRP2[11] and Irr,[12] suggesting that $HO2_{tail}{}^R$ also binds heme at the HRMs with Cys ligation. Heme binding to $HO2_{tail}{}^R$ was additionally confirmed by EPR spectroscopy (Figure 1B). Fe^{3+}-$HO2_{tail}{}^R$ displayed a low-spin signal (signal Y) with rhombic *g* values g = [2.41, 2.26, and 1.91], identical to the signal previously observed for Fe^{3+}-$HO2_{sol}{}^R$.[7,9]

The ability of $HO2_{tail}{}^R$ to ligate heme in a manner independent of the catalytic binding site provided further evidence of a multiple-binding site model in $HO2_{sol}{}^R$. To quantitatively determine the number of Fe^{3+}-heme binding sites, $HO2_{sol}{}^O$ was treated with TCEP and, after separation from TCEP, incubated with excess Fe^{3+}-heme. After removal of unbound Fe^{3+}-heme, the pyridine hemochrome assay demonstrated that indeed Fe^{3+}-$HO2_{sol}{}^R$ bound 2.1 ± 0.1 hemes per monomer of protein. Further, the absorbance spectrum of the heme-bound form of Fe^{3+}-$HO2_{sol}{}^R$ included a band at 406 nm and a shoulder at 368 nm (Figure 1A). The spectrum appears to be a composite of the spectra of Fe^{3+}-$HO2_{core}$, a variant that lacks the HRM region, and of Fe^{3+}-$HO2_{tail}{}^R$ (Figure 1A). Therefore, the binding of heme to $HO2_{tail}{}^R$ and the binding of 2.1 hemes to $HO2_{sol}{}^R$ provide strong evidence of a multiple-binding site model in which heme binds to the core of the protein via His45 and, in a separate binding event, to the HRMs.

ENDOR and EPR Experiments Confirm Coordination of the Axial Nitrogen to Fe^{3+}-Heme in HO2

Previous EPR experiments demonstrated that Fe^{3+}-$HO2_{sol}{}^R$ displayed signal Y with rhombic *g* values g = [2.41, 2.26, 1.91] and a second low-spin signal (signal X) with

rhombic g values g = [2.87, 2.26, 1.63], while Fe^{3+}-$HO2_{sol}^{O}$ displayed only signal X.[7,9] Now that we have shown here that Fe^{3+}-$HO2_{tail}^{R}$ displays signal Y and that Fe^{3+}-$HO2_{sol}^{R}$ binds two Fe^{3+}-hemes per monomer of protein, the two Fe^{3+}-$HO2_{sol}^{R}$ signals can be explained by a model in which one heme binds to the core of the protein via His45/aquo (signal X) and a second heme binds to the HRMs (signal Y). The assignment of cysteine ligation for signal Y was presented in the previous ^{1}H ENDOR study.[9] However, the same report also demonstrates that the Fe^{3+}-heme associated with signal Y does not have an aquo (H_xO) ligand,[9] leaving the other ligand unidentified. Because the g values of signal Y are consistent with His/Cys ligation,[26,27] histidine was suspected to play a role in Fe^{3+}-heme ligation.

To confirm the histidyl ligation of signal X and identify the second axial ligand of Y, we acquired the Davies ENDOR spectra of Fe^{3+}-$HO2_{sol}^{R}$, Fe^{3+}-$HO2_{sol}^{O}$, and Fe^{3+}-$HO2_{tail}^{R}$ with both the ^{14}N- and ^{15}N-labeled polypeptide, where in all samples the ferriheme pyrroles contain ^{14}N (Figure 2). In the frequency range of 4–7 MHz, the ENDOR spectra of all samples are dominated by the ^{14}N responses from the four in-plane pyrrole nitrogens. At the single-crystal-like field (g_1 = 2.87) for X, the ENDOR spectra of [^{15}N]-Fe^{3+}-$HO2_{sol}^{O}$, [^{15}N]-Fe^{3+}-$HO2_{sol}^{R}$, and [^{14}N]-Fe^{3+}-$HO2_{sol}^{R}$ all exhibit a quadrupole-split ^{14}N doublet signal from these nitrogens [splitting, $3P(^{14}N) \approx 1$ MHz; $A(^{14}N) \sim 6$ MHz]. The spectra for both [^{15}N]-Fe^{3+}-$HO2_{sol}^{O}$ and [^{15}N]-Fe^{3+}-$HO2_{sol}^{R}$ show an additional ^{15}N peak at $\nu_+ = 8.7$ MHz that is absent in the unlabeled ([^{14}N]-Fe^{3+}-$HO2_{sol}^{R}$) sample. This frequency corresponds to a hyperfine coupling $A(^{15}N)$ of ~10 MHz; this coupling is mostly isotropic [$A_{iso}(^{15}N) \sim 10$ MHz] as derived from the two-dimensional ENDOR pattern collected across the full EPR spectrum (Figure 1 of the Supporting Information). The coupling also corresponds to an $A_{iso}(^{14}N)$ of ~7 MHz, as calculated from the ratio of the nuclear g factors; $|g_n(^{15}N)/g_n(^{14}N)| = 1.4 = |A(^{15}N)/A(^{14}N)|$. The natural-abundance [^{14}N]-Fe^{3+}-$HO2_{sol}^{R}$ sample is not visible in the corresponding ^{14}N response because it is buried under the signals from the pyrroles. These measurements demonstrate that the low-spin ferriheme of signal X seen for the full enzyme has a nitrogenous axial ligand in both Fe^{3+}-$HO2_{sol}^{O}$ and Fe^{3+}-$HO2_{sol}^{R}$, consistent with the assignment of His45 as a Fe^{3+}-heme ligand in the core of HO2 based on structural studies.[4]

The ENDOR spectra collected at the higher field of g_1 = 1.91 for [^{15}N]-Fe^{3+}-$HO2_{sol}^{R}$ and [^{14}N]-Fe^{3+}-$HO2_{sol}^{R}$, where both X and Y contribute to the EPR intensity, show a poorly resolved ^{14}N signal at 6–8 MHz from the heme pyrroles of both X and Y centers. In addition, the spectrum of [^{15}N]-Fe^{3+}-$HO2_{sol}^{R}$ shows not one but two $\nu_+(^{15}N)$ features, at $\nu_+(^{15}N) \sim 8$ and 10.5 MHz. Spectra taken at multiple fields across the EPR signal (Figure 1 of the Supporting Information) show that the signal at $\nu_+(^{15}N) = 10.5$ MHz at g = 1.91 correlates with the feature at g = 2.87 assigned to His45 of signal X. Moreover, this signal is absent for [^{15}N]Fe^{3+}-$HO2_{tail}^{R}$, which does not include the region of the HO2 polypeptide that spans His45.

The second ^{15}N signal in the g = 1.91 ENDOR spectrum of [^{15}N]-Fe^{3+}-$HO2_{sol}^{R}$, at $\nu_+(^{15}N) \sim 8$ MHz (which corresponds to a ^{14}N hyperfine coupling A of ~3–4 MHz), can then be assigned to a nitrogenous ligand of the signal Y Fe^{3+}-heme. This peak also is present in the ENDOR spectrum from signal Y of [^{15}N]-Fe^{3+}-$HO2_{tail}^{R}$. Because Fe^{3+}-$HO2_{tail}^{R}$ does not

include the region of HO2 that spans His45, this signal must be assigned to a histidine in the tail region of HO2 (residues 213– 288). His256 is the only histidine in both Fe^{3+}-$HO2_{tail}^{R}$ and Fe^{3+}-$HO2_{sol}^{R}$, leading us to conclude that His256 is acting as a Fe^{3+}-heme ligand in $HO2^{R}$.

We note that it is not surprising that the hyperfine couplings of the axial histidyl nitrogens in the low-spin heme sites X and Y are not identical (His45, 6–7 MHz; His256, 3–4 MHz), given that these Fe^{3+}-hemes are undoubtedly six-coordinate, with different axial ligand "partners". The ferric heme of X has His45/H_xO ligation, but that of Y has His256/Cys coordination. The fact that the ^{14}N hyperfine coupling in Y is smaller than that in X is expected, given that a small coupling was reported previously[28] for the proximal nitrogen of the histidine of the myoglobin–mercaptoaethanol complex (Fe-His/Cys coordination). Overall, these results thus confirm that one Fe^{3+}-heme binds to the core with His/H_xO ligation and strongly suggest that a second Fe^{3+}-heme binds to the tail with His/Cys ligation.

His45 Is Not Necessary for Binding of Fe^{3+}-Heme to $HO2^{R}$

A previous hypothesis[7] had suggested a ligand exchange event could be occurring upon reduction of the disulfide bond in $HO2_{sol}$. In the model that was proposed, Fe^{3+}-heme would remain bound to the catalytic core via His45, and upon reduction of the disulfide bond, a cysteine residue from one of the HRMs could displace one of the Fe^{3+}-heme ligands. The ENDOR experiments described above, in conjunction with those published previously,[9] strongly suggest Cys/His ligation of Fe^{3+}-heme bound to $HO2_{sol}^{R}$. Despite the evidence presented above for the multiple-binding site model, the ENDOR results presented here also demonstrate nitrogen ligation, leaving open the possibility of a Fe^{3+}-heme ligated by His45 and Cys that could occur upon a ligand exchange event. Therefore, the H45A variant of $HO2_{sol}$ was constructed to test the ligand exchange model. The EPR spectrum of Fe^{3+}-$HO2_{sol}(H45A)^{R}$ was recorded (Figure 1B). The Fe^{3+}-$HO2_{sol}(H45A)^{R}$ displayed signal Y, identical to that of Fe^{3+}-$HO2_{tail}^{R}$. The results confirm the role of another His in Fe^{3+}-heme binding and that the His/Cys binding site in the tail part of HO2 is independent of the His45/aquo binding site. However, the results cannot rule out the possibility that a His45/Cys-ligated heme is transiently formed in wild-type $HO2^{R}$.

Identification of Fe^{3+}-Heme Ligands in $HO2^{R}$

$HO2_{tail}$ contains two cysteines, both of which (Cys265 and Cys282) are associated with an HRM. While previous experiments have confirmed the interaction of Cys265 with Fe^{3+}-heme, the same experiments were less conclusive about the interaction of Cys282 with Fe^{3+}-heme.[9] Therefore, the participation of the two cysteines in Fe^{3+}-heme binding was investigated. C265A and C282A variants of $HO2_{tail}$ were treated with TCEP to ensure reduction of any cysteine sulfenate[7] or intermolecular disulfide bonds and, after separation from TCEP, incubated with excess Fe^{3+}-heme. After removal of unbound Fe^{3+}-heme, the protein was subjected to a pyridine hemochrome assay, which demonstrated that the C265A and C282A variants of Fe^{3+}-$HO2_{tail}^{R}$ contained 0.74 ± 0.03 and 0.8 ± 0.2 heme per monomer of protein, respectively. The absorbance spectra of the two variants were, however, very distinct (Figure 3A). The spectrum of Fe^{3+}-$HO2_{tail}(C265A)^{R}$ displayed a broad band at 368 nm, consistent with spectra reported for other proteins that bind heme at a

HRM.[11,12] In contrast, the spectrum of the Fe^{3+}-$HO2_{tail}(C282A)^R$ variant included a peak at 422 nm with a shoulder at 360 nm.

The features displayed in the absorbance spectrum of Fe^{3+}-$HO2_{tail}(C282A)^R$ are reminiscent of the spectral features observed for proteins in which cysteine and histidine are important for heme ligation, including HRI,[14,15] consistent with the ENDOR results presented above. As $HO2_{tail}$ contains just one histidine (His256), $HO2_{tail}(H256A/C282A)^R$ was analyzed for heme binding. The H256A/C282A variant still bound heme (0.83 ± 0.03 heme per monomer), suggesting His256 is not necessary for heme binding. However, the spectrum of Fe^{3+}-$HO2_{tail}(H256A/C282A)^R$ is very distinct from that of Fe^{3+}-$HO2_{tail}(C282A)^R$; Fe^{3+}-$HO2_{tail}(H256A/C282A)^R$ displayed an absorbance peak at 368 nm rather than at 422 nm (Figure 3B). Thus, when present, His256 and Cys265 are both involved in coordinating heme. The spectrum of Fe^{3+}-$HO2_{tail}(H256A/C265A)^R$ was indistinguishable from that of Fe^{3+}-$HO2_{tail}(C265A)^R$ (Figure 3C), suggesting no role for His256 in the binding of heme with Cys282. Further, $HO2_{tail}(C265A/C282A)^R$ did not bind Fe^{3+}-heme (data not shown), demonstrating that His256 cannot alone bind Fe^{3+}-heme, i.e., in a manner independent of Cys265. Thus, it appears as though there are two binding modes within $HO2_{tail}^R$: one with Cys265 and His256 and another with Cys282.

The EPR spectra of the variants of Fe^{3+}-$HO2_{tail}^R$ are consistent with the ligand assignments made on the basis of the absorbance spectra (Figure 4). The EPR spectrum of the heme-bound form of Fe^{3+}-$HO2_{tail}(C282A)^R$ displays a low-spin signal with g = [2.41, 2.26, and 1.91], identical to that observed for Fe^{3+}-$HO2_{tail}^R$ (signal Y). ENDOR spectroscopy confirmed that signal Y is associated with Cys/His ligation (see above), in agreement with the assignment of Cys265 and His256 as ligands. In addition, upon further substitution of His256 with alanine to create Fe^{3+}-$HO2_{tail}(H256A/C282A)^R$, the low-spin signal is shifted to g = [2.51, 2.29, 1.86]. This signal is similar that observed for Fe^{3+}-$HO2_{tail}(C265A)^R$ and Fe^{3+}-$HO2_{tail}(H256A/C265A)^R$ (g = [2.48, 2.28, and 1.89] for both), and the values are consistent with those reported for IRP2, another protein that binds heme at a HRM.[11]

The ability to bind Fe^{3+}-heme at both of the C-terminal HRMs in wild-type $HO2_{tail}^R$ is not, however, readily apparent in the EPR spectra. The EPR spectra of Fe^{3+}-$HO2_{tail}^R$ and Fe^{3+}-$HO2_{tail}(C282A)^R$ are nearly identical (signal Y), with no apparent contribution of the spectrum of Fe^{3+}-$HO2_{tail}(C265A)^R$ to the spectrum of the wild type. Thus, the EPR spectra could suggest that Cys265, but not Cys282, binds heme in wild-type $HO2_{tail}^R$. However, several explanations can be offered. The intensity of the Fe^{3+}-HO2 $(C282A)^R$ signal is much greater than that of Fe^{3+}-HO2 $(C265A)^R$, suggesting that, in the spectrum of Fe^{3+}-$HO2_{tail}^R$, the contribution of Fe^{3+}-heme bound to Cys282 may be masked by the more intense signal of Fe^{3+}-heme bound to Cys265. In addition, temperature-dependent changes in the absorbance spectrum of Fe^{3+}-$HO2_{tail}^R$ illustrate that as the temperature is decreased, the population of Fe^{3+}-heme bound to His256/Cys265 is increased, which is indicated by the increase in absorbance at 422 nm (Figure 5). Therefore, the much lower temperatures at which the EPR spectra are recorded may be low enough to completely or, nearly so, favor Fe^{3+}-heme binding via Cys265 and His256 over binding via Cys282. Lastly, a difference in binding affinity between the two sites could lead to preferential binding of Fe^{3+}-heme to one site (see below).

Fe^{3+}-Heme Binding Affinity for HO2

The data presented above suggest that $HO2_{sol}^{R}$ contains multiple heme binding sites. A reasonable hypothesis to explain the fact that binding to the second binding site has not been previously identified is that there is a significant difference in the binding affinities for the two sites. Indeed, when $HO2_{core}$ was titrated with Fe^{3+}-heme, a plot of the heme difference spectra revealed a K_d of 0.014 ± 0.004 μM (Figure 6 and Table 1). However, Fe^{3+}-heme difference titrations with $HO2_{tail}(C282A)^{R}$ and $HO2_{tail}(C265A)^{R}$ revealed K_d values of 0.09 ± 0.03 and 0.9 ± 0.3 μM, respectively (Figure 6). In addition, a Fe^{3+}-heme difference titration with $HO2_{sol}^{R}$ revealed binding of Fe^{3+}-heme to the core before a significant amount of Fe^{3+}-heme bound to the HRMs (Figure 6), consistent with the differences in K_d values obtained for $HO2_{sol}^{O}$ and the variants of $HO2_{tail}^{R}$. However, the K_d values for each of the binding sites on $HO2_{sol}^{R}$ and $HO2_{tail}^{R}$ were difficult to determine with accuracy from the titration data because of the complexity of the spectra. Therefore, kinetic measurement of the on and off rates for Fe^{3+}-heme binding were independently measured. Given that the K_d for Fe^{3+}-heme measured by difference absorbance spectroscopy is well below the concentration of protein in the assay, the kinetic measurements also should provide more accurate binding/dissociation constants.

The Fe^{3+}-heme off rates (k_{-heme}) were measured using the apo-H64Y/V68F-myoglobin ("green heme") assay.[23] In this assay, one can clearly distinguish between the spectrum of Fe^{3+}-heme bound to the "green" myoglobin (with extremely tight binding) and that of Fe^{3+}-heme bound to HO2. Fe^{3+}-HO2 was prepared as described above by incubating the oxidized or TCEP-reduced protein with excess Fe^{3+}-heme followed by removal of unbound Fe^{3+}-heme. Fe^{3+}-HO2 was subsequently incubated with apo-H64Y/V68F-myoglobin while the increase in the absorbance at 600 due to Fe^{3+}-heme scavenging by apo-H64Y/V68F-myoglobin was being monitored. The results for Fe^{3+}-$HO2_{core}$ were fit to a single-exponential association function with a rate constant of 0.0012 ± 0.00004 s^{-1} (Table 1).

In contrast, the results for Fe^{3+}-$HO2_{tail}^{R}$ fit best to a double-exponential function, with a fast phase of 0.0086 ± 0.003 s^{-1} (32%) and a slow phase of 0.0023 ± 0.0004 s^{-1}. These two phases were assigned on the basis of the results of the assay with the C265A and C282A variants of Fe^{3+}-$HO2_{tail}^{R}$, which yielded off rates of 0.0055 ± 0.0005 and 0.0023 ± 0.0001 s^{-1}, respectively. Therefore, it appears that Fe^{3+}-$HO2_{tail}^{R}$ has a fast off rate because of the dissociation of heme from Cys282 and a slower off rate because of the dissociation of heme from Cys265. The measured off rates for the two HRM binding sites are very similar to that reported for HRI (0.0015 s^{-1}), another protein that binds Fe^{3+}-heme at a HRM.[15]

The rate constants determined for Fe^{3+}-$HO2_{core}$ and Fe^{3+}-HO_{tail}^{R} were then used to interpret the results for Fe^{3+}-$HO2_{sol}^{R}$. The time course fit best to a double-exponential function, with a slow rate constant of 0.00054 ± 0.00006 s^{-1} and a fast rate constant of 0.0031 ± 0.0002 s^{-1} (62%). Because the rate constant for the slow phase approximated that observed for $HO2_{sol}^{O}$, we presume that this reflects Fe^{3+}-heme that has dissociated from His45 at the core of the protein. The other, faster phase was consistent with the rate for dissociation of heme from Cys265. A third phase, likely caused by dissociation of heme from Cys282, was not observed. One possibility is that the low occupancy of the Cys282 site

leads to a small absorbance change that is masked by that of the other two binding sites of HO2. Another possibility is that dissociation of Fe^{3+}-heme from Cys282 at such a fast rate results in locally high concentrations of free Fe^{3+}-heme around HO2. This scenario could provide the other binding sites on HO2 an opportunity to bind Fe^{3+}-heme before apo-H64Y/V68F-myoglobin despite having a weaker affinity for Fe^{3+}-heme, and the dissociation from Cys282 would not be observed in the assay. Either way, these results suggest that Fe^{3+}-heme binds tightly to the core of $HO2^{O}$ and $HO2^{R}$, but more loosely to HRM1 (His256/Cys265) and very loosely to HRM2 (Cys282) at the tail.

To accurately determine the K_d values by kinetic measurements, the Fe^{3+}-heme on rates were measured. The heme on rates were determined by performing stopped flow spectroscopy experiments under anaerobic conditions. The binding of Fe^{3+}-heme to HO2 was monitored at 406 nm with increasing concentrations of $HO2_{core}$, $HO2_{tail}$ $(C282A)^{R}$ or $HO2_{sol}{}^{R}$. Binding to Cys282 was not monitored in these experiments because the absorbance of the Fe^{3+}-heme-bound species is very low at 406 nm and its maximal absorbance at 368 nm significantly overlaps with the spectrum of free Fe^{3+}-heme.

For each variant analyzed, k_{obs} displayed a hyperbolic dependence on apoprotein concentration (Figure 7). As described previously for other proteins,[29,30] the hyperbolic dependence indicates a two-step binding process in which a Fe^{3+}-heme–apoprotein reversible complex precedes axial coordination (see Scheme 1). If k_1 and k_2 are much greater than k_{coord} and $k_{\_heme}$ is much smaller than k_{coord}, the dependence of k_{obs} on apoprotein concentration can be described by eq 1.

$$k_{\mathrm{obs}}=\frac{k_{\mathrm{coord}}\,[\mathrm{apoprotein}]}{\frac{k_2}{k_1}+[\mathrm{apoprotein}]} \quad (1)$$

Fits of eq 1 to the plot of k_{obs} versus apoprotein concentration yielded values for k_2/k_1 and k_{coord} of 14.1 ± 0.3 μM and 91 ± 1 s^{-1} for $HO2_{core}$ and 14 ± 4 μM and 110 ± 10 s^{-1} for $HO2_{tail}(C282A)^{R}$, respectively. The apparent second-order rate constants [$k'_{heme} \approx k_{coord}/(k_2/k_1)$] are thus 6.4 and 7.6 μM^{-1} s^{-1} for $HO2_{core}$ and $HO2_{tail}(C282A)^{R}$, respectively. The small difference in the heme on rates for the two variants was also reflected in the results of similar analysis of the data for $HO2_{sol}{}^{R}$ in which we measured the k_{obs} versus the concentration of observable binding sites available on the apoprotein (instead of apoprotein concentration). Binding at either His45 or Cys265 results in absorbance changes at 406 nm in $HO2_{sol}{}^{R}$, as demonstrated by experiments with $HO2_{core}$ and $HO2_{tail}(C282A)^{R}$, yielding two observable binding sites per monomer of $HO2_{sol}{}^{R}$. The fitted values for k_2/k_1 and k_{coord} were and 9.1 ± 0.7 μM and 63 ± 1 s^{-1} for $HO2_{core}$, respectively, yielding a single apparent second-order rate constant, k'_{heme}, of 6.9 μM^{-1} s^{-1}. It therefore appears that both binding sites (at His45 in the core and Cys265 in the tail of $HO2_{sol}{}^{R}$ have very similar heme on rates. Further, the on rates are very similar to the rates reported for other heme binding proteins, including HRI[15] and myoglobin,[31] which generally show less variation in on rates than in off rates.

The calculated dissociation equilibrium constants ($k_{\text{-heme}}$ from the apo-H64Y/V68F-myoglobin assay divided by k'_{heme}) are thus approximately 0.00008–0.0001 μM for binding

of Fe^{3+}-heme to the core at His45 and 0.0003–0.0004 μM for binding of Fe^{3+}-heme to the tail at Cys265 (Table 1). The difference titrations suggested K_d values weaker than those calculated from these experiments. However, dissociation constants from the kinetic and equilibrium measurements have slightly different interpretations, with the kinetic measurements putting more of an emphasis on the individual events rather than the more global perspective of events observed in the equilibrium experiments. Regardless, the results of the kinetic experiments suggest a 2–5-fold difference in binding affinity between the sites, and similarly, the Fe^{3+}-heme difference titrations suggested an ~6-fold difference. Therefore, the results of both methods suggest a significant difference in binding affinity between the two sites.

Further, despite the lack of observation of a rate of dissociation from Cys282 in the assay with Fe^{3+}-$HO2_{sol}^{R}$, the results demonstrate the applicability of using the variants to dissect the events occurring in the more full-length version of the protein. For instance, the rate of dissociation assigned to the Cys265 site remains relatively consistent between Fe^{3+}-$HO_{tail}(C282A)^{R}$ (0.0023 ± 0.0001 s^{-1}), Fe^{3+}-HO_{tail}^{R} (0.0023 ± 0.0004 s^{-1}), and Fe^{3+}-$HO2_{sol}^{R}$ (0.0031 ± 0.0002 s^{-1}). In addition, the rate of dissociation assigned to the His45 site in the core of the protein also remains relatively unchanged between the oxidized and reduced forms of $HO2_{sol}$ (Fe^{3+}-$HO2_{core}$, 0.0012 ± 0.00004 s^{-1}; Fe^{3+}-$HO2_{sol}^{R}$, 0.00054 ± 0.00006 s^{-1}). In summary, the results highlight the fact that the binding events at the core and the tail appear to be independent of each other and occur with significantly different binding affinities because of the rate of heme dissociation.

DISCUSSION

HRMs, short amino acid stretches containing a Cys-Pro dipeptide, are increasingly found to be involved in modulating the activity of heme binding proteins through the binding of heme. HO2 contains three HRMs, and mounting mutational and spectroscopic evidence confirms that the cysteines found in the HRMs of $HO2^{R}$ are involved in Fe^{3+}-heme ligation. Therefore, it is of great interest to determine if and how the HRMs are involved in HO2 function.

Insight into the relationship between the HRMs and HO2 function can be garnered by determining how the HRMs of $HO2^{R}$ bind Fe^{3+}-heme. Previous models include a fishhook mechanism in which a cysteine residue from one of the HRMs could displace one of the ligands (His45 or aquo) of Fe^{3+}-heme bound to the catalytic core upon reduction of the disulfide bond.[7] Alternatively, Maines and co-workers have proposed a multiple-binding site model in which the HRMs form a Fe^{3+}-heme binding site that is independent of the catalytic site.[16] A recent spectroscopic study of HO2 favored the multiple-binding site model.[9] Now, the results presented here offer confirmation of this model, provide insights into the role(s) of the multiple binding sites on $HO2^{R}$, and distinguish HO2 from HO1, which lacks HRMs and binds only a single heme.

Here, we demonstrate the existence of a redox-regulated second Fe^{3+}-heme binding site on HO2 that is available only upon reduction of a disulfide bond between Cys265 and Cys282. Both $HO2_{tail}^{R}$ and $HO2_{sol}(H45A)^{R}$ were shown to bind Fe^{3+}-heme despite not having

access to the key ligand at the catalytic site because of the truncation of the protein and mutation of the catalytic site histidine necessary for Fe^{3+}-heme ligation, respectively. Fe^{3+}-$HO2_{sol}(H45A)^{R}$ and Fe^{3+}- $HO2_{tail}^{R}$ share the same spectral features, suggesting that both constructs bind Fe^{3+}-heme with the same ligands at a site that is independent of the catalytic site. Fe^{3+}-$HO2_{sol}^{R}$ exhibits these same spectral features but, in addition, has signals that are the same as Fe^{3+}-$HO2_{sol}^{O}$. The fact that Fe^{3+}-$HO2_{sol}^{R}$ has both sets of features offers support for the multiple-binding site model.

Also demonstrated here, and further supporting the multiple-binding site model, is the ability of Fe^{3+}-$HO2_{sol}^{R}$ to bind 2.1 ± 0.1 hemes per monomer of protein. A previous study had suggested that $HO2_{sol}^{R}$ binds only one heme per monomer of protein, leading to the proposal of the fishhook mechanism.[7] However, the calculation was based a Fe^{3+}-heme difference titration of $HO2_{sol}^{R}$ presented here would also indicate one Fe^{3+}-heme per monomer. However, binding of Fe^{3+}-heme to the HRMs does not significantly alter the absorbance at 406 nm, suggesting that previous experiments may not have detected the other binding events. Further, although the spectral changes occurring upon ligation of heme to $HO2_{tail}^{R}$ are quite prominent, the changes are at 370 nm where they could have readily been mistaken for the accumulation of unbound heme (maximal absorbance at 385 nm) rather than identified as another binding event. Tryptophan fluorescence quenching has also been used to determine the binding affinity of $HO2_{sol}^{R}$ and similarly suggested the binding of one Fe^{3+}-heme.[8] While this method detected binding of Fe^{3+}-heme to the catalytic site, it appears to be ineffective in observing binding of Fe^{3+}-heme to the HRM sites. This may in part be due to the fact that the construct used in that study (spanning residues 1–293) contained only one tryptophan, Trp121. Trp121 is located in the core of the protein, so it may not have been able to detect a binding event at the HRMs because of their location in the highly mobile tail region of HO2.

In the characterization of the HRM binding sites, binding of Fe^{3+}-heme to Cys265 and Cys282 was expected on the basis of previous studies. However, the participation of His256 in Fe^{3+}-heme binding had not been predicted. His256 is outside the region (residues 262–271, human HO2 numbering) encompassed by the Cys265-containing peptide studied by Maines and co-workers.[16] The Cys265-containing peptide displayed an absorbance maximum of 369 nm upon incubation with Fe^{3+}-heme in the Maines study, while the absorbance spectrum of Fe^{3+}-$HO2_{tail}^{R}$ reported here included a shoulder at 422 nm in addition to a broad band at 368 nm. The differences between the spectra are slight, and the work presented here using mutagenesis and spectroscopic techniques was required to identify the participation of His256 in Fe^{3+}-heme ligation. Interestingly, Cys265 can ligate Fe^{3+}-heme both with and without His256. This scenario is reminiscent of that described for HRI in which Fe^{3+}-heme ligates to the Cys of an HRM both with and without a His residue located in a completely different domain of the protein.[14,15] In the case of HRI, heme regulation of the protein is due to global structural changes induced by Fe^{3+}-heme ligation with residues from different domains. Structural changes have also been recently suggested for HO2 as the HRM-containing region is proposed to dock to the core of the protein upon Fe^{3+}-heme binding.[9] The docking model has not yet been shown to be dependent on His256, however, so the role of His256 in relation to HO2 function is not immediately evident.

Clearly, there is a redox component to the function of the HRMs because the disulfide bond must be reduced before heme can bind. In addition, heme bound to the HRMs could be used as a sensor of gaseous molecules such as NO or CO. The HRMs have previously been implicated in NO sensing.[32] Another possibility is that the HRM sites are involved in heme sensing. The differing affinities among the three potential sites on HO2 (His45/aquo, His256/Cys265, and Cys282) would poise HO2 to sense varying heme levels, perhaps even acting as storage sites for Fe^{3+}-heme before being degraded by HO2. In fact, it has recently been noted that the highly mobile region of HO2 in which the HRMs are located may dock to the core of the protein,[9] providing a fairly reasonable mechanism for the direct transfer of Fe^{3+}-heme from the HRMs to the core. Even if it is not a direct transfer mechanism, the binding of heme to these sites has the potential to keep local concentrations of Fe^{3+}-heme high, facilitating rapid turnover by the catalytic core of HO2.

The results presented here implicate the HRMs as an important factor in HO2 function. Given that HO1 lacks HRMs, or in fact any Cys residues, it also indicates that redox regulation of heme binding is a feature unique to HO2. Further investigation into the exact nature of the role the HRM binding sites will perhaps offer more clarity into what distinguishes HO2 from HO1 and the role of each in heme homeostasis. Further, the findings could contribute to a more general understanding of HRMs of other heme binding proteins and their potential link to the redox state of the cell.

Supplementary Material

Refer to Web version on PubMed Central for supplementary material.

Acknowledgments

Funding Support was provided by Grants R01-HL-102662A (S.W.R.) and R01-GM-111097 (B.M.H.) from the National Institute of General Medical Sciences (NIGMS) and in part by NIGMS Grant T32 GM007215 (A.M.S.).

ABBREVIATIONS

HO2	heme oxygenase-2
HRM	heme regulatory motif
$HO2_{sol}$	HO2 spanning residues 1–288
$HO2_{tail}$	HO2 spanning residues 213–288;
$HO2_{core}$	HO2 spanning residues 1–248;
$HO2^{O}$	HO2 containing a disulfide bond between Cys265 and Cys282
$HO2^{R}$	HO2 in the disulfide bond-reduced form
Fe^{3+}-HO2	Fe^{3+}-heme-bound HO2
HO1	heme oxygenase-1
IRP2	iron regulatory protein 2
Irr	bacterial iron response regulator protein

HRI	heme-regulated eukaryotic initiation factor 2α (heme-regulated inhibitor)
EPR	electron paramagnetic resonance
ENDOR	electron nuclear double resonance
TCEP	tris(2-carboxyethyl)phosphine

REFERENCES

(1). Maines MD. The heme oxygenase system: A regulator of second messenger gases. Annu. Rev. Pharmacol. Toxicol. 1997; 37:517–554. [PubMed: 9131263]

(2). Maines MD, Trakshel GM, Kutty RK. Characterization of two constitutive forms of rat liver microsomal heme oxygenase: Only one molecular species of the enzyme is inducible. J. Biol. Chem. 1986; 261:411–419. [PubMed: 3079757]

(3). McCoubrey WK, Maines MD. Domains of rat heme oxygenase-2: The amino terminus and histidine-151 are required for heme oxidation. Arch. Biochem. Biophys. 1993; 302:402–408. [PubMed: 8489244]

(4). Bianchetti CM, Yi L, Ragsdale SW, Phillips GN Jr. Comparison of apo- and heme-bound crystal structures of a truncated human heme oxygenase-2. J. Biol. Chem. 2007; 282:37624–37631. [PubMed: 17965015]

(5). Schuller DJ, Wilks A, de Montellano PRO, Poulos TL. Crystal structure of human heme oxygenase-l. Nat. Struct. Biol. 1999; 6:860–867. [PubMed: 10467099]

(6). Yi L, Jenkins PM, Leichert LI, Jakob U, Martens JR, Ragsdale SW. Heme regulatory motifs in heme oxygenase-2 form a thiol/disulfide redox switch that responds to the cellular redox state. J. Biol. Chem. 2009; 284:20556–20561. [PubMed: 19473966]

(7). Yi L, Ragsdale SW. Evidence that the heme regulatory motifs in heme oxygenase-2 serve as a thiol/disulfide redox switch regulating heme binding. J. Biol. Chem. 2007; 282:21056–21067. [PubMed: 17540772]

(8). Varfaj F, Lampe JN, de Montellano PRO. Role of cysteine residues in heme binding to human heme oxygenase-2 elucidated by two-dimensional NMR spectroscopy. J. Biol. Chem. 2012; 287:35181–35191. [PubMed: 22923613]

(9). Bagai I, Sarangi R, Fleischhacker AS, Sharma A, Hoffman BM, Zuiderweg ERP, Ragsdale SW. Spectroscopic studies reveal that the heme regulatory motifs of heme oxygenase-2 are dynamically disordered and exhibit redox-dependent interaction with heme. Biochemistry. 2015 DOI: 10.1021/bi501489r.

(10). Gardner JD, Yi L, Ragsdale SW, Brunold TC. Spectroscopic insights into axial ligation and active-site H-bonding in substrate-bound human heme oxygenase-2. JBIC, J. Biol. Inorg. Chem. 2010; 15:1117–1127.

(11). Ishikawa H, Kato M, Hori H, Ishimori K, Kirisako T, Tokunaga F, Iwai K. Involvement of heme regulatory motif in heme-mediated ubiquitination and degradation of IRP2. Mol. Cell. 2005; 19:171–181. [PubMed: 16039587]

(12). Ishikawa H, Nakagaki M, Bamba A, Uchida T, Hori H, O'Brian MR, Iwai K, Ishimori K. Unusual heme binding in the bacterial iron response regulator protein: Spectral characterization of heme binding to the heme regulatory motif. Biochemistry. 2011; 50:1016–1022. [PubMed: 21192735]

(13). Qi ZH, Hamza I, O'Brian MR. Heme is an effector molecule for iron-dependent degradation of the bacterial iron response regulator (Irr) protein. Proc. Natl. Acad. Sci. U.S.A. 1999; 96:13056–13061. [PubMed: 10557272]

(14). Igarashi J, Murase M, Iizuka A, Pichierri F, Martinkova M, Shimizu T. Elucidation of the heme binding site of heme-regulated eukaryotic initiation factor 2 α kinase and the role of the regulatory motif in heme sensing by spectroscopic and catalytic studies of mutant proteins. J. Biol. Chem. 2008; 283:18782–18791. [PubMed: 18450746]

(15). Miksanova M, Igarashi J, Minami M, Sagami I, Yamauchi S, Kurokawa H, Shimizu T. Characterization of heme-regulated eIF2 α kinase: Roles of the N-terminal domain in the oligomeric state, heme binding, catalysis, and inhibition. Biochemistry. 2006; 45:9894–9905. [PubMed: 16893190]

(16). McCoubrey WK, Huang TJ, Maines MD. Heme oxygenase-2 is a hemoprotein and binds heme through heme regulatory motifs that are not involved in heme catalysis. J. Biol. Chem. 1997; 272:12568–12574. [PubMed: 9139709]

(17). Aslanidis C, Dejong PJ. Ligation-independent cloning of PCR products (LIC-PCR). Nucleic Acids Res. 1990; 18:6069–6074. [PubMed: 2235490]

(18). Stols L, Gu MY, Dieckman L, Raffen R, Collart FR, Donnelly MI. A new vector for high-throughput, ligation-independent cloning encoding a tobacco etch virus protease cleavage site. Protein Expression Purif. 2002; 25:8–15.

(19). Zhou P, Wagner G. Overcoming the solubility limit with solubility-enhancement tags: Successful applications in biomolecular NMR studies. J. Biomol. NMR. 2010; 46:23–31. [PubMed: 19731047]

(20). Spencer ALM, Bagai I, Becker DF, Zuiderweg ERP, Ragsdale SW. Protein/protein interactions in the mammalian heme degradation pathway: Heme oxygenase-2, cyto-chrome P450 reductase, and biliverdin reductase. J. Biol. Chem. 2014; 289:29836–29858. [PubMed: 25196843]

(21). Dawson, RMC. Data for Biochemical Research. 3rd ed. Clarendon Press; New York: 1986.

(22). Berry EA, Trumpower BL. Simultaneous determination of hemes *a*, *b*, and *c* from pyridine hemochrome spectra. Anal. Biochem. 1987; 161:1–15. [PubMed: 3578775]

(23). Hargrove MS, Singleton EW, Quillin ML, Ortiz LA, Phillips GN, Olson JS, Mathews AJ. His64(E7)→ Tyr apomyoglobin as a reagent for measuring rates of hemin dissociation. J. Biol. Chem. 1994; 269:4207–4214. [PubMed: 8307983]

(24). Ascoli F, Fanelli MR, Antonini E. Preparation and properties of apohemoglobin and reconstituted hemoglobins. Methods Enzymol. 1981; 76:72–87. [PubMed: 7329287]

(25). Owens CP, Du J, Dawson JH, Goulding CW. Characterization of heme ligation properties of Rv0203, a secreted heme binding protein involved in *Mycobacterium tuberculosis* heme uptake. Biochemistry. 2012; 51:1518–1531. [PubMed: 22283334]

(26). Davydov R, Sudhamsu J, Lees NS, Crane BR, Hoffman BM. EPR and ENDOR characterization of the reactive intermediates in the generation of NO by cryoreduced oxy-nitric oxide synthase from Geobacillus stearothermophilus. J. Am. Chem. Soc. 2009; 131:14493–14507. [PubMed: 19754116]

(27). Flanagan HL, Gerfen GJ, Lai A, Singel DJ. Orientation-selective ^{14}N electron-spin echo envelope modulation (ESEEM): The determination of ^{14}N quadrupole coupling tensor principal axis orientations in orientationally disordered solids. J. Chem. Phys. 1988; 88:2162–2168.

(28). Magliozzo RS, Peisach J. Evaluation of nitrogen nuclear hyperfine and quadrupole coupling parameters for the proximal imidazole in myoglobin azide, myoglobin cyanide, and myoglobin mercaptoethanol complexes by electron-spin echo envelope modulation spectroscopy. Biochemistry. 1993; 32:8446–8456. [PubMed: 8395204]

(29). Yukl ET, Jepkorir G, Alontaga AY, Pautsch L, Rodriguez JC, Rivera M, Moenne-Loccoz P. Kinetic and spectroscopic studies of hemin acquisition in the hemophore HasAp from *Pseudomonas aeruginosa*. Biochemistry. 2010; 49:6646–6654. [PubMed: 20586423]

(30). Nygaard TK, Blouin GC, Liu M, Fukumura M, Olson JS, Fabian M, Dooley DM, Lei B. The mechanism of direct heme transfer from the streptococcal cell surface protein shp to HtsA of the HtsABC transporter. J. Biol. Chem. 2006; 281:20761–20771. [PubMed: 16717094]

(31). Hargrove MS, Barrick D, Olson JS. The association rate constant for heme binding to globin is independent of protein structure. Biochemistry. 1996; 35:11293–11299. [PubMed: 8784183]

(32). Ding Y, McCoubrey WK, Maines MD. Interaction of home oxygenase-2 with nitric oxide donors: Is the oxygenase an intracellular `sink' for NO? Eur. J. Biochem. 1999; 264:854–861. [PubMed: 10491133]

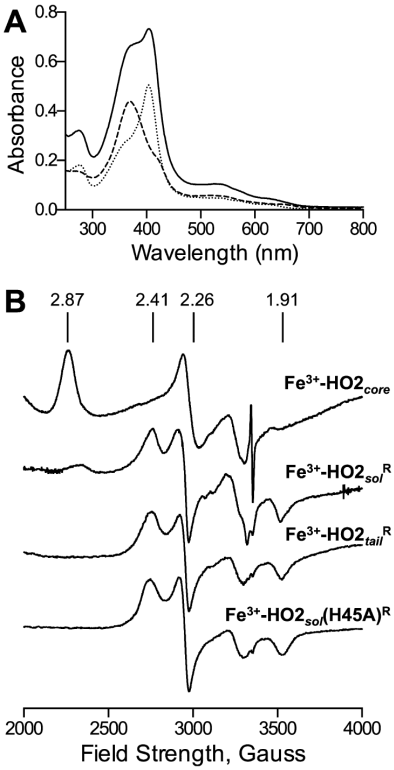

Figure 1.

Characterization of HO2 in the Fe^{3+}-heme-bound forms. (A) Absorbance spectra of 5 μM Fe^{3+}-$HO2_{core}$ (…), Fe^{3+}-$HO2_{tail}^{R}$ (---), or Fe^{3+}-$HO2_{sol}^{R}$ (—) in 50 mM Tris (pH 8.0) and 50 mM KCl at 20 °C. (B) EPR spectra of Fe^{3+}-$HO2_{core}$, Fe^{3+}-$HO2_{tail}^{R}$, Fe^{3+}-$HO2_{sol}^{R}$, and Fe^{3+}-$HO2_{sol}(H45A)^{R}$. Samples were prepared and run as described (see Methods). The *g* values are indicated above the spectra.

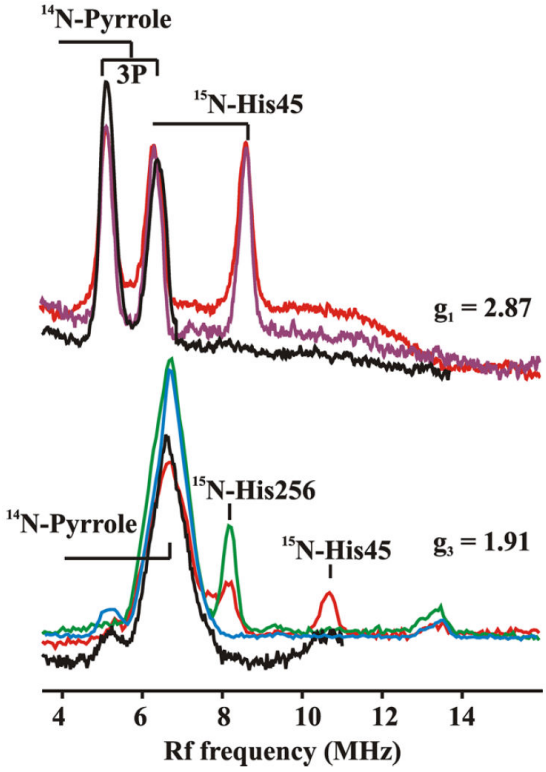

Figure 2.

^{14}N and ^{15}N DAVIES ENDOR spectra of unlabeled and ^{15}N-labeled Fe^{3+}-HO2 measured at the indicated *g* values. Spectra were recorded of ^{15}N-labeled Fe^{3+}-$HO2_{sol}^{R}$ (red), ^{15}N-labeled Fe^{3+}-$HO2_{sol}^{O}$ (purple), unlabeled Fe^{3+}-$HO2_{sol}^{R}$ (black), unlabeled Fe^{3+}-$HO2_{tail}^{R}$ (blue), and ^{15}N-labeled Fe^{3+}-$HO2_{sol}^{R}$ (green). Experimental conditions: MW frequency of 34.7 GHz, *T* of 2 K, pulse sequence described in Methods, tp of 40 ns, τ of 600 ns, trf of 30 μs, trep of 50 ms, and 256 transients/scan.

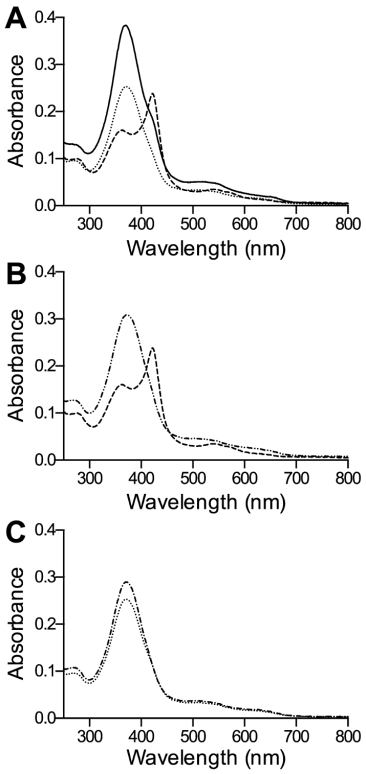

Figure 3.

Absorbance spectra of wild-type Fe^{3+}-$HO2_{tail}^{R}$ and its variants. Spectra were recorded at 20 °C in 50 mM Tris (pH 8.0) and 50 mM KCl with a protein concentration of 5 μM. (A) Wild-type Fe^{3+}-$HO2_{tail}^{R}$ (—), Fe^{3+}-$HO2_{tail}$(C265A)^{R} (…), and Fe^{3+}-$HO2_{tail}$(C282A)^{R} (---). (B) Fe^{3+}-$HO2_{tail}$(C282A)^{R} (---) and Fe^{3+}-$HO2_{tail}$(H256A/C282A)^{R} (·-·). (C) Fe^{3+}-$HO2_{tail}$(C265A)^{R} (---) and Fe^{3+}-$HO2_{tail}$(H256A/C265A)^{R} (·-·).

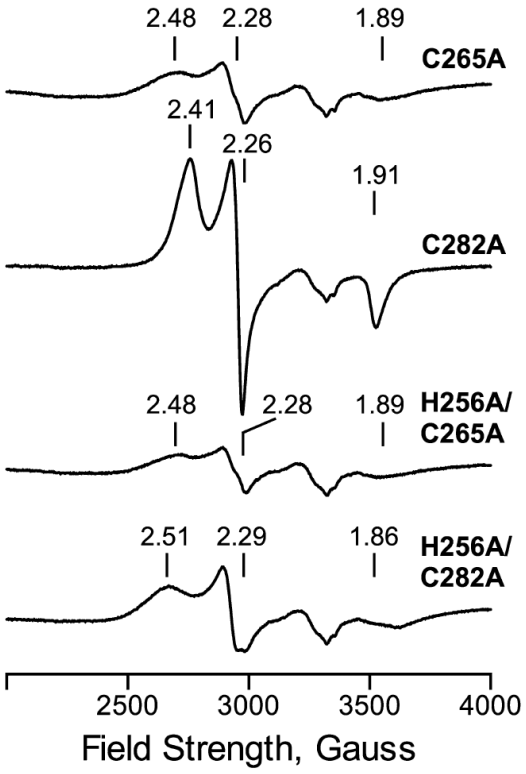

Figure 4.

EPR spectra of Fe^{3+}-$HO2_{tail}^{R}$ variants. Samples were prepared and run as described (see Methods). The *g* values are indicated above the spectra of Fe^{3+}-$HO2_{tail}$(C265A)^{R}, Fe^{3+}-$HO2_{tail}$(C282A)^{R}, Fe^{3+}-$HO2_{tail}$(H256A/C265A)^{R}, and Fe^{3+}-$HO2_{tail}$(H256A/C282A)^{R}.

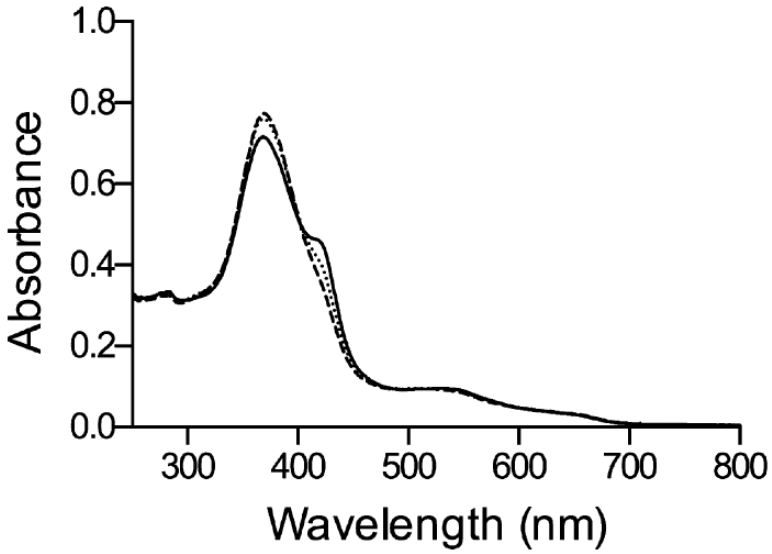

Figure 5.

Temperature dependence of Fe^{3+}-$HO2_{tail}^{R}$. The absorbance spectrum of 5 μM Fe^{3+}-$HO2_{tail}^{R}$ in 50 mM Tris (pH 8.0) and 50 mM KCl was recorded at 35 (---), 20 (…), and 5 °C (—).

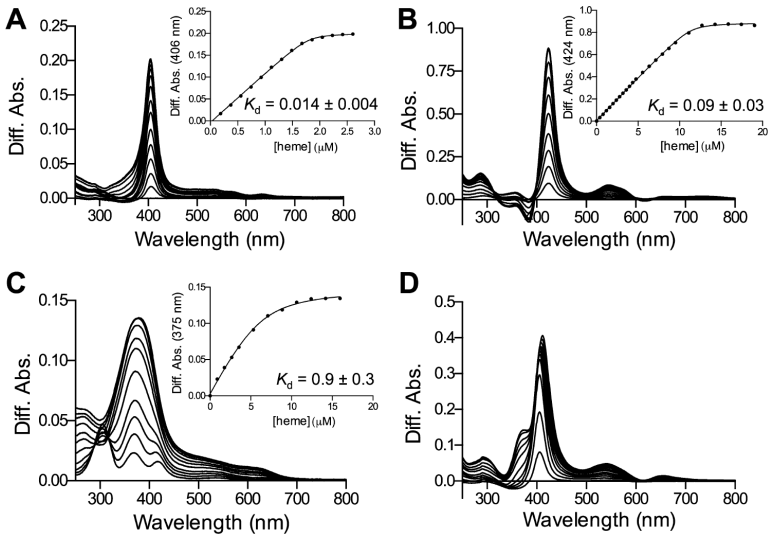

Figure 6.

Fe^{3+}-heme difference titrations with $HO2_{core}$, $HO2_{tail}(C282A)^R$, $HO2_{tail}(C265A)^R$, and $HO2_{sol}{}^R$. Difference titrations were performed in 50 mM Tris (pH 8.0) and 50 mM KCl at 20 °C under anaerobic conditions with (A) 2 μM $HO2_{core}$, (B) 10 μM $HO2_{tail}(C282A)^R$, (C) 6 μM $HO2_{tail}(C265A)^R$, or (D) 5 μM $HO2_{sol}{}^R$. Insets in panels A–C are plots of the respective data at the indicated wavelength with the solid lines representing the fits to the quadratic equation to obtain K_d values.

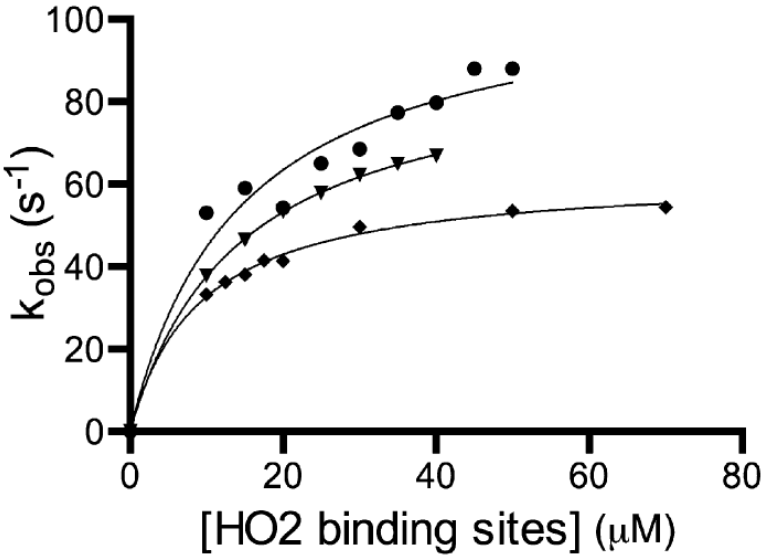

Figure 7.

Plot of observed rate constants as a function of the concentration of available Fe^{3+}-heme binding sites on HO2. The apo form of $HO2_{core}$ (▼), $HO2_{tail}(C282A)^{R}$ (●), or $HO2_{sol}^{R}$ (◆) was mixed at various concentrations with Fe^{3+}-heme in a stopped-flow instrument within an anaerobic chamber. Data were collected at 20 °C while monitoring was conducted at 406 nm. The data were fit to eq 1 as described in the text, and the resulting fits are represented as solid lines.

$$\mathrm{HO2} + \mathrm{Fe^{3+}\text{-}heme} \underset{k_2}{\overset{k_1}{\rightleftharpoons}} \mathrm{HO2{:}Fe^{3+}\text{-}heme} \underset{k_{\text{-heme}}}{\overset{k_{\text{coord}}}{\rightleftharpoons}} \mathrm{Fe^{3+}\text{-}HO2}$$

Scheme 1.
Binding of Fe^{3+}-Heme to HO2

Table 1

Rate and Equilibrium Constants for Binding of Fe^{3+}-Heme to HO2

	$k_{\text{-heme}}$ (s^{-1})	k'_{heme} ($\mu M^{-1}\ s^{-1}$)	K_d (μM) ($k_{\text{-heme}}/k'_{\text{heme}}$)	K_d (μM) (titrations)
$HO2_{core}$	0.0012 ± 0.00004	6.4	0.0002	0.014 ± 0.004
$HO2_{tail}(C282A)^R$	0.0023 ± 0.0001	7.6	0.0003	0.09 ± 0.03
$HO2_{tail}(C265A)^R$	0.0055 ± 0.0005	ND[a]	ND[a]	0.9 ± 0.3
$HO2_{tail}^R$	0.0023 ± 0.0004	ND[a]	ND[a]	ND[a]
	0.0086 ± 0.003 (32%)			
$HO2_{sol}^R$	0.00054 ± 0.00006	6.9	0.0004	ND[a]
	0.0031 ± 0.0002 (62%)		0.00008	

[a]Value not determined.